



Contents lists available at ScienceDirect

## Bioorganic &amp; Medicinal Chemistry Letters

journal homepage: [www.elsevier.com/locate/bmcl](http://www.elsevier.com/locate/bmcl)

## N-aryl-piperidine-4-carboxamides as a novel class of potent inhibitors of MALT1 proteolytic activity

Achim Schlapbach\*, Laszlo Revesz, Carole Pissot Soldermann, Thomas Zoller, Catherine H. Régnier, Frédéric Bornancin, Thomas Radimerski, Jutta Blank, Ansgar Schuffenhauer, Martin Renatus, Paulus Erbel, Samu Melkko, Richard Heng, Oliver Simic, Ralf Endres, Markus Wartmann, Jean Quancard

Novartis Institutes for BioMedical Research, CH-4002 Basel, Switzerland

## ARTICLE INFO

## Article history:

Received 20 February 2018

Revised 16 April 2018

Accepted 8 May 2018

Available online xxxxx

## Keywords:

MALT1

Paracaspase

Protease inhibitors

Autoimmune disease

B-cell lymphoma

## ABSTRACT

Starting from a weak screening hit, potent and selective inhibitors of the MALT1 protease function were elaborated. Advanced compounds displayed high potency in biochemical and cellular assays. Compounds showed activity in a mechanistic Jurkat T cell activation assay as well as in the B-cell lymphoma line OCI-Ly3, which suggests potential use of MALT1 inhibitors in the treatment of autoimmune diseases as well as B-cell lymphomas with a dysregulated NF- $\kappa$ B pathway. Initially, rat pharmacokinetic properties of this compound series were dominated by very high clearance which could be linked to amide cleavage. Using a rat hepatocyte assay a good *in vitro-in vivo* correlation could be established which led to the identification of compounds with improved PK properties.

© 2018 Elsevier Ltd. All rights reserved.

The NF- $\kappa$ B pathway is of chief importance in immunity and cancer biology.<sup>1</sup> Attempts to target this pathway by small molecule inhibitors have had little success so far, essentially because NF- $\kappa$ B is required for tissue homeostasis, in particular in the liver.<sup>2</sup> As a consequence, full blockade of this pathway turned out to be associated with toxicities which prevented therapeutic use of this concept.<sup>2</sup> Mucosa-associated lymphoid tissue lymphoma translocation protein 1 (MALT1) plays a key role in NF- $\kappa$ B pathway activation, in particular in T and B lymphocytes.<sup>3,4</sup> Upon antigen receptor stimulation, MALT1 is recruited to CARD11 (CARMA1) together with BCL10 to form the 'CBM' complex that triggers inhibitor of kappa-B kinase (IKK) activation. Akin to the structurally related caspases, MALT1 (aka paracaspase 1) possesses an original cysteine protease domain. However, in contrast to caspases, MALT1 cleaves substrates at arginine residues.<sup>5</sup> X-ray crystal structures of the MALT1 catalytic domain show a dimeric organization in a classical caspase-like fold.<sup>6</sup> Several studies using mouse models of MALT1 deficiencies have shown that MALT1 plays a role in autoimmune diseases.<sup>7</sup> Furthermore, first MALT1 inhibitors and their activity *in vitro* and in animal models have been disclosed.<sup>8</sup> Collectively, this provides evidence to support MALT1 as an attractive novel protease target for development of small molecule inhibitors with

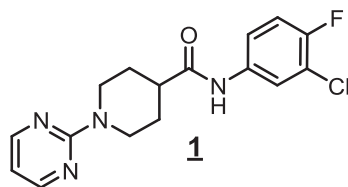
the potential to dampen NF- $\kappa$ B signaling in B-cell lymphomas and autoimmune diseases.<sup>9</sup>

Following the discovery of MALT1's protease function and its key role in lymphocyte signaling<sup>3</sup> a high throughput screen was initiated to search for compounds which inhibit the cleavage of an artificial MALT1 substrate.<sup>10</sup> In addition to several known, mostly irreversible, cysteine protease inhibitors, compound **1** devoid of any classical covalent warhead functionality was discovered (Fig. 1). We observed that **1** not only inhibited the MALT1 protease function *in vitro* with an IC<sub>50</sub> of 1.6  $\mu$ M, but that it also displayed activity in a cellular reporter gene assay (RGA), measuring NF- $\kappa$ B activation in a HEK293 reporter cell line stably transfected with the fusion protein cIAP2-MALT1.<sup>10,11</sup> Furthermore, compound **1** inhibited the cleavage of one of the MALT1 substrates, BCL10 in the OCI-Ly3 cell line which is characterized by constitutive CBM assembly, resulting in high spontaneous MALT1 activity.<sup>12,13</sup> Based on these results an optimization campaign was initiated.

For SAR studies the molecule was derivatized in three major parts, the piperidine substituents, the core piperidine moiety and the amide substituent. Substituted benzenes and 6-ring heterocycles were tolerated as piperidine substituents (Table 1). Aliphatic N-substituents or a benzyl group led to inactive molecules (compounds **4** and **5**). The pyrimidine as it is present in the hit structure could be replaced by a phenyl-, a pyridyl- or pyridazyl-ring (compounds **2**, **3** and **10**). Substitution in *meta*-position led to reduced

\* Corresponding author.

E-mail address: [achim.schlapbach@novartis.com](mailto:achim.schlapbach@novartis.com) (A. Schlapbach).



|                       |                   |
|-----------------------|-------------------|
| MALT1 biochemical:    | 1.6 $\mu\text{M}$ |
| MALT1 cellular (RGA): | 3.1 $\mu\text{M}$ |
| BCL10 cleavage:       | 5.4 $\mu\text{M}$ |
| Solubility pH 6.8:    | 21 $\mu\text{M}$  |
| cLogP:                | 2.3               |

Fig. 1. Chemical structure and properties of HTS hit compound 1.

potency (compound **6**); however a significant increase in potency was achieved by adding *ortho*-substituents, in particular lipophilic substituents like chlorine (compound **8**). Interestingly, the same increase in potency could be achieved by addition of an *ortho* amino group (compound **9**). With the exception of compound **8** which appears to be unexpectedly potent in our biochemical assay, biochemical activity generally translated well into cellular potency as measured in a NF- $\kappa$ B reporter gene assay, or more directly, by measuring inhibition of cleavage of the MALT1 substrate BCL10.

An aromatic group was required as amide substituent, as compound **11** containing a cyclohexyl substituent was devoid of any activity while the unsubstituted phenyl derivative **12** retained

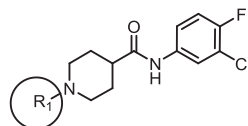
potency (Table 2). Lipophilic substituents, e.g. a chlorine in the *meta*-position increased potency tremendously (compound **13**). The *para*-position was very tolerant of modifications and several substitutions could lead to further potency increase. As such a *para* fluoro- or methoxy-group yielded potent inhibitors (**8** and **14**, respectively) and a triazole (1,2,3 or 1,2,4) was found to be the most beneficial *para*-substituent (compounds **15–18**). The triazole substituent could be further substituted, e.g. by an additional amide as in **18**. *Ortho*-substituents were not tolerated (not shown), and the phenyl ring could be replaced by a 3-pyridyl-substituent without major impact on potency, e.g. **16** vs. **17**.

With potent MALT1 inhibitors at hand we turned our attention to analyzing their cellular effects. To assess the effects on T cell activation, selected compounds were tested using an IL-2 reporter gene assay in Jurkat T cells after stimulation with PMA/anti-CD28 monoclonal antibody (mAb).<sup>10</sup> In line with the compounds' effect on the protease function of MALT1, the IL-2 reporter gene was inhibited in the 50–100 nM range (Table 3).

In addition, compounds inhibited OCI-Ly3 cell proliferation with IC<sub>50</sub> values in the low micromolar range, whereas proliferation of BJAB cells, which do not display constitutive MALT1/NF- $\kappa$ B activity was not affected, indicating that the anti-proliferative effect is linked to MALT1 inhibition<sup>14</sup> (Table 3).

Off-target activity of compound **17** was assessed in an extended selectivity panel. Apart from weak activity (8  $\mu\text{M}$ ) on Cox-2, no significant activity was found in a panel of 64 receptors, transporters and enzymes. In particular, only very high micromolar activity was noted in a panel of cysteine proteases.<sup>15</sup>

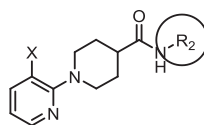
Table 1  
SAR around the piperidine substituent.



|           | R <sub>1</sub> | MALT1 biochemical IC <sub>50</sub> ( $\mu\text{M}$ ) | MALT1 cellular NF- $\kappa$ B RGA IC <sub>50</sub> ( $\mu\text{M}$ ) | MALT1 cellular BCL10 cleavage EC <sub>50</sub> ( $\mu\text{M}$ ) |
|-----------|----------------|--|--|--|
| <b>1</b>  |                | 1.62   | 3.1  | 5.4  |
| <b>2</b>  |                | 0.82   | 3.2  | 9.2  |
| <b>3</b>  |                | 1.90   | n.d.   | n.d.   |
| <b>4</b>  |                | >100   | n.d.   | n.d.   |
| <b>5</b>  |                | >100   | n.d.   | n.d.   |
| <b>6</b>  |                | 9.0  | n.d.   | n.d.   |
| <b>7</b>  |                | 0.42   | 2.7  | 2.1  |
| <b>8</b>  |                | 0.028  | 1.35   | 1.5  |
| <b>9</b>  |                | 0.10   | 0.42   | 0.54   |
| <b>10</b> |                | 0.10   | 0.29   | 0.40   |

For detailed assay descriptions see [10,13]. The IC<sub>50</sub> values are averages of at least 2 separate determinations.

**Table 2**  
SAR around the amide substituent.



|           | R <sub>2</sub> | X               | MALT1 biochemical IC <sub>50</sub> (μM) | MALT1 cellular NF-κB RGAIC <sub>50</sub> (μM) | MALT1 cellular BCL10 cleavage EC <sub>50</sub> (μM) |
|-----------|----------------|-----------------|---|---|---|
| <b>11</b> |                | Cl              | >100                                    | n.d.  | n.d.  |
| <b>12</b> |                | Cl              | 4.7                                     | n.d.  | n.d.  |
| <b>13</b> |                | Cl              | 0.21                                    | 1.59  | 3.4   |
| <b>8</b>  |                | Cl              | 0.028                                   | 1.35  | 1.5   |
| <b>14</b> |                | Cl              | 0.013                                   | 0.19  | 0.45  |
| <b>15</b> |                | Cl              | 0.004                                   | 0.09  | 0.23  |
| <b>16</b> |                | NH <sub>2</sub> | 0.007                                   | 0.09  | 0.56  |
| <b>17</b> |                | NH <sub>2</sub> | 0.035                                   | 0.11  | 0.19  |
| <b>18</b> |                | Cl              | 0.021                                   | 0.14  | 0.21  |

For detailed assay descriptions see [10,13]. The IC<sub>50</sub> values are averages of at least 2 separate determinations.

**Table 3**  
Cellular profile of selected MALT1 inhibitors.

|  | <b>15</b> | <b>16</b> | <b>17</b> |
|--|-----------|-----------|-----------|
| NF-κB RGA, IC <sub>50</sub> [μM]             | 0.09      | 0.09      | 0.11      |
| BCL10 cleavage, EC <sub>50</sub> [μM]        | 0.23      | 0.56      | 0.19      |
| OCY-Ly3 proliferation, EC <sub>50</sub> [μM] | 1.40      | 3.60      | 2.0       |
| BJAB proliferation, EC <sub>50</sub> [μM]    | >10       | >10       | >10       |
| IL-2 RGA, IC <sub>50</sub> [μM]              | 0.05      | 0.08      | n.d.      |

The high selectivity and the non-protease-inhibitor-like structure prompted us to investigate the binding mode of this inhibitor class. By SPR (surface plasmon resonance spectroscopy) reversible binding could be demonstrated. Similar as shown for Phenothiazin derivatives<sup>16</sup> binding of compound **17** to an E397A mutant MALT1 was reduced, which suggests these inhibitors also bind in the recently discovered allosteric pocket at the interface of the catalytic and the Ig3 domain.<sup>16</sup>

Next, we evaluated the compounds with respect to their ADME profile and pharmacokinetic properties. In general compounds were characterized by good permeability and moderate to high microsomal *in vitro* clearance (Table 4).

Solubility was low to moderate at neutral pH and higher at pH4 as expected for these slightly basic molecules. Rat pharmacokinetics revealed very high *in vivo* clearance, e.g. for compounds **17** and **18**. In particular the *in vivo* clearance of **18** was higher than what could be expected from the *in vitro* microsomal clearance alone.

This high clearance could be attributed to cleavage of the central amide bond *in vivo*, as high levels of acid **24** (see Scheme 2) were detected in blood samples upon re-analysis.<sup>17</sup> Furthermore compounds were stable in plasma and whole blood, indicating that the proteolytic activity responsible for this amide cleavage was not present in blood. In order to establish an *in vitro* assay to better mimic the *in vivo* stability we tested selected structurally diverse compounds in rat hepatocytes which might contain enzymes responsible for the amide cleavage.<sup>18</sup> Indeed, rat hepatocyte clearance correlated much better with *in vivo* clearance for this diverse set of compounds (Fig. 2).

Thus, compound **18** showed a much higher turn-over in hepatocytes, better reflecting the *in vivo* situation. Compound **19** displayed high turnover in both *in vitro* systems which translated to very high clearance *in vivo*. For compound **20** low clearance was found in microsomes as well as in hepatocytes translating into good PK properties with a moderate rat *in vivo* clearance of 43 ml·min<sup>-1</sup>·kg<sup>-1</sup>, bioavailability of 46% but a short half-life of 0.5 h. Most remarkable was the shift from moderate clearance in microsomes to low clearance in hepatocytes for compound **21**. The *in vitro* *in vivo* correlation for compound **21** using hepatocytes was much better, translating to a rat *in vivo* clearance of 56 ml·min<sup>-1</sup>·kg<sup>-1</sup>, moderate bioavailability of 46% and a half-life of 2.4 h (Table 4). While there is no clear rationale for this improvement based on the chemical structures, the *in vitro* hepatocyte assay could be used to further optimize *in vivo* clearance. However, compounds with good *in vivo* exposure, e.g. **20** and **21** were only moderately active

**Table 4**  
*In vitro* ADME and *in vivo* parameters for selected compounds.

|   | 17         | 18         | 19        | 20         | 21        |
|---|------------|------------|-----------|------------|-----------|
| MALT1 IC <sub>50</sub> /NF-κB RGA [μM]                          | 0.035/0.11 | 0.021/0.14 | 0.054/3.7 | 0.184/0.64 | 0.340/3.0 |
| <i>in vitro</i>   |            |            |           |            |           |
| Solubility pH4/6.8 [μM]   | 48/<4      | 8/<4       | <4/<4     | 170/7      | 690/16    |
| Caco-2 Papp A-B [10 <sup>-6</sup> cm/s]                         | 19.4       | 8.2        | n.d.      | n.d.       | 7.2       |
| PAMPA Permeability, log Pe [cm/s]                               | -4.4       | -5.3       | -4.0      | -6.2       | -4.2      |
| RLM Cl [mL·min <sup>-1</sup> ·kg <sup>-1</sup> ]                | 102        | 59.8       | 81.0      | 29.0       | 60.2      |
| Rat hepatocyte Cl [μL·min <sup>-1</sup> ·10 <sup>6</sup> cells] | n.d.       | 228        | 173       | 4.1        | 18.8      |
| <i>in vivo</i> (rat)  |            |            |           |            |           |
| CL [mL·min <sup>-1</sup> ·kg <sup>-1</sup> ]                    | 259        | 282        | 320       | 43         | 56        |
| V <sub>ss</sub> [L/kg]  | 4.1        | 7.5        | 21.4      | 1.1        | 8.7       |
| t <sub>1/2</sub> [h]  | 0.3        | 0.6        | 2.0       | 0.5        | 2.4       |
| AUC i.v., (1 mg/kg) [nM·h]                                      | 161        | 125        | 143       | 914        | 623       |
| BAV [%]   | n.d.       | n.d.       | n.d.      | 46         | 46        |

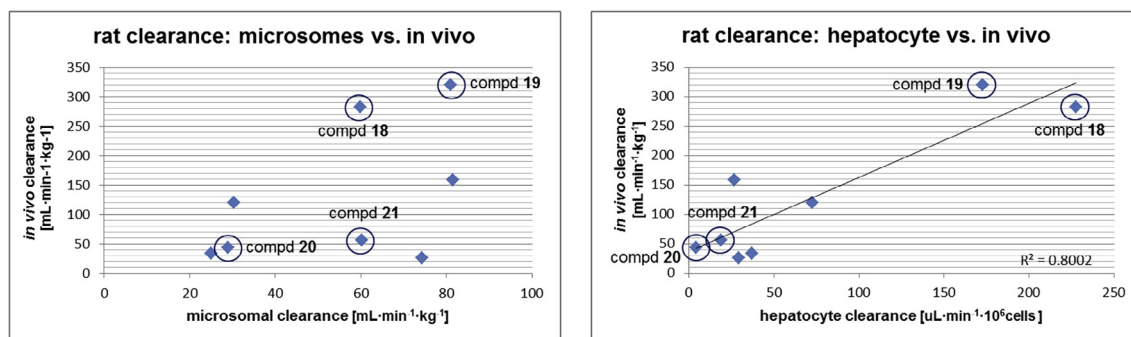
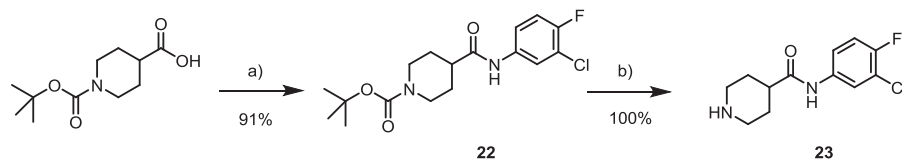


**Fig. 2.** Correlation of microsomal clearance, hepatocyte clearance and rat *in vivo* clearance.

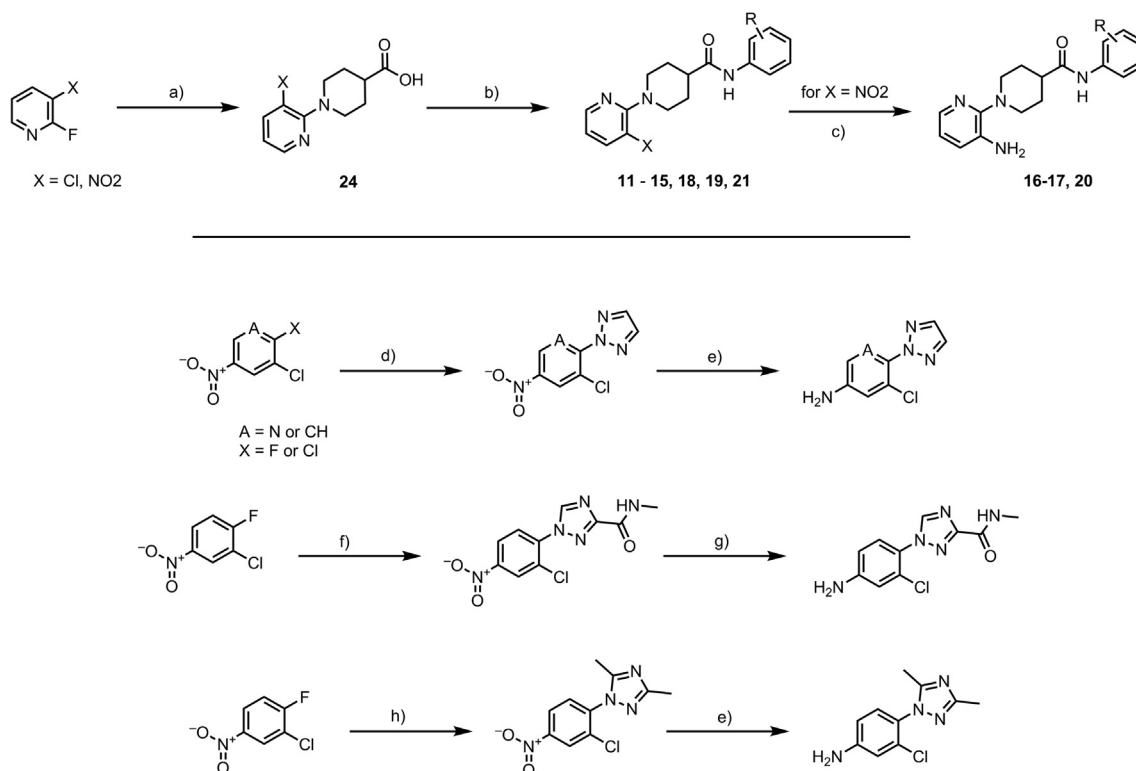


reagents and conditions for step c):

| compd# | reactant                  | conditions   | yield [%] |
|--------|---------------------------|--|-----------|
| 1      | 2-chloropyrimidine        | DIPEA, DMF 100°C   | 35        |
| 2      | bromobenzene              | Xphos, Pd(OAc) <sub>2</sub> , Cs <sub>2</sub> CO <sub>3</sub> , tBuOH, 100°C | 44        |
| 3      | 2-bromopyridine           | BINAP, Pd <sub>2</sub> (dba) <sub>3</sub> , NaOtBu, toluene 80 °C            | 21        |
| 6      | 4-cyano-2-chloropyridine  | BINAP, Pd <sub>2</sub> (dba) <sub>3</sub> , NaOtBu, toluene 80 °C            | 8         |
| 7      | 3-cyano-2-fluoropyridine  | DIPEA, NMP 160°C, microwave  | 72        |
| 8      | 3-chloro-2-fluoropyridine | DIPEA, NMP 160°C, microwave  | 41        |
| 9      | 2-fluoro-3-nitropyridine  | DIPEA, NMP 160°C, microwave  | 89        |
| 10     | 2,3-dichloropyrazine      | DIPEA, NMP 145°C, microwave  | 77        |

R =  
 p-fluorobenzyl **4**  
 i-butyl **5**

**Scheme 1.** Synthesis of compounds **1–10**, reagents and conditions: a) TBTU, DIPEA, DMF r.t. (91%); b) 4 N HCl in dioxane, r.t. (100%); c) see table; d) aldehyde, NaBH<sub>3</sub>CN, MeOH/AcOH, DIPEA, r.t. (39–40%).



**Scheme 2.** Synthesis of compounds **11–21**, reagents and conditions: a) piperidine-4-carboxylic acid, DIPEA, NMP, 120–180 °C (microwave) (82–92%); b) aniline/aminopyridine, HATU, DIPEA, DMF, r.t., or EDC, DCM, r.t. (29–75%); c) SnCl<sub>2</sub>, 2 N HCl, ethanol, reflux (62–94%); d) 1,2,3-triazole, NaH, DMF, 0 °C (24–35%), e) SnCl<sub>2</sub>, 2 N HCl, ethanol, reflux (83–91%); f) *N*-methyl-1H-1,2,4-triazole-3-carboxamide, K<sub>2</sub>CO<sub>3</sub>, DMF, r.t. (93%); g) Fe, NH<sub>4</sub>Cl, ethanol, reflux (69–84%); h) 3,5-dimethyl-1,2,4-triazole, NaH, DMF, 0 °C (68%).

on MALT1 which did not allow to progress a compound into *in vivo* efficacy studies and the optimization of this scaffold was discontinued.

Compounds were synthesized using the reaction sequences depicted in Schemes 1 and 2.

Amide coupling of Boc-piperidine carboxylic acid with anilines provided amides **22**, which upon de-protection yielded the piperidines **23**. Finally, the piperidine substituent was installed using Buchwald-type couplings,<sup>19</sup> direct S<sub>N</sub>Ar or reductive amination to provide compounds **1–10**.

Variations to the amide substituent could be best achieved using the route shown in Scheme 2.

Nucleophilic substitution of 2-fluoropyridines with piperidine carboxylic acid, followed by amide coupling provided compounds **11–15** and **18, 19, 21**. In case of compounds **16, 17** and **20** further reduction of the nitro group yielded the final compounds (Scheme 2). Non-commercial anilines and aminopyridines were prepared by nucleophilic substitution of fluoro- or chloro-nitrobenzenes and pyridines respectively, followed by nitro reduction using either SnCl<sub>2</sub> or iron.

In summary, we discovered novel, highly selective MALT1 protease inhibitors which display high potency in biochemical and cellular assays. Compounds showed activity in a mechanistic T cell activation assay (IL-2 RGA) in Jurkat T cells as well as in the lymphoma cell line OCI-Ly3, which suggests potential use of MALT1 inhibitors in the treatment of autoimmune diseases as well as B-cell lymphomas with a dysregulated NF-κB pathway. Initially, rat pharmacokinetic properties were dominated by very high clearance which could be linked to amide cleavage. Using a rat hepatocyte assay to guide optimization and compound selection, compounds with improved PK properties were identified. With the excellent potency and selectivity profile these compounds

could serve as good *in vitro* tool compounds to study MALT1 biology. However, it was not possible to identify a compound combining sufficient potency and good pharmacokinetic properties which would allow to further progress this compound series.

## A. Supplementary data

Supplementary data associated with this article can be found, in the online version, at <https://doi.org/10.1016/j.bmcl.2018.05.017>.

## References

- (a) Bacher S, Schmitz ML. *Curr Pharm Des.* 2004;10:2827; (b) Lawrence T. *Cold Spring Harb. Perspect Biol.* 2009;1:a001651; (c) Zubair A, Frieri M. *Curr Allergy Asthma Rep.* 2013;13:44.
- Bamborough P, Morse MA, Ray KP. *Drug News Perspect.* 2010;23:483–490.
- (a) Rebeaud F, Hailfinger S, Posevitz-Fejfar A, et al. *Nat Immunol.* 2008;9:272; (b) Coornaert B, Baens M, Heynincx K, et al. *Nat Immunol.* 2008;9:263.
- (a) For recent reviews see: Jaworski M, Thome M. *Cell Mol Life Sci.* 2016;73:459; (b) Rosebeck S, Rehman AO, Lucas PC, McAllister-Lucas LM. *Cell Cycle.* 2011;10:2485.
- (a) Uren AG, O'Rourke K, Aravind LA, Pisabarro MT, Seshagiri S, Koonin EV, Dixit VM. *Mol. Cell.* 2000; 6: 961.; (b) Hachmann J, Snipas SJ, van Raam BJ, et al. *Biochem J.* 2012;443:287.
- (a) Hachmann J, Snipas SJ, van Raam BJ, et al. *Biochem J.* 2012;443:287; (b) Wiesmann C, Leder L, Blank J, et al. *J Mol Biol.* 2012;419:4.
- (a) Brüstle A, Brenner D, Knobbe CB, Mak TW, et al. *J Clin Invest.* 2012;122:4698; (b) Mc Guire C, Wieghofer P, Elton L, Muylaert D, Prinz M, Beyaert R, Van Loo G. *J Immunol.* 2013;6:2896; (c) Liu W, Guo W, Hang N, et al. *Oncotarget.* 2016;7:30536.
- (a) Nagel D, Spranger S, Vincendeau M, et al. *Cancer Cell.* 2012;22:825; (b) Fontan L, Yang C, Kabaleeswaran V, et al. *Cancer Cell.* 2012;22:812; (c) Mc Guire C, Elton L, Wieghofer P, et al. *J Neuroinflamm.* 2014;11:124; (d) Liu W, Guo W, Hang N, et al. *Oncotarget.* 2016;7:30536; (e) Lim SM, Jeong Y, Lee S, et al. *J Med Chem.* 2015;58:8491.
- (a) McAllister-Lucas LM, Baens M, Lucas PC. *Clin. Cancer Res.* 2011; 17: 6623, for recent reviews.;

- (b) Jaworski M, Thome M. *Cell Mol Life Sci.* 2016;73:459;  
(c) Juillard M, Thome M. *Curr Opin Hematol.* 2016;23:402.
10. (a) For detailed assay descriptions see: Pissot Soldermann C, Quancard J, Schlapbach A, Simic O, Tintelnot-Blomley M, Zoller T, PCT Int. Appl. WO 2015181747, Kammertoens K, Quancard J, Schlapbach A, Simic O, Tintelnot-Blomley M, Woollam G, PCT Int. Appl. WO 2017081641.;  
(b) Bardet M, Unterreiner A, Malinverni C, et al. The T-cell fingerprint of MALT1 paracaspase revealed by selective inhibition. *Immunol Cell Biol.* 2018;96:81–99.
  11. Noels H, van Loo G, Hagens S, et al. *J Biol Chem.* 2007;282:10180.
  12. Lenz G, Davis RE, Ngo VN, et al. *Science.* 2008;319:1676.
  13. MALT1-dependent BCL10 cleavage is assessed in a capture ELISA format using the MSD (Meso Scale Discovery) platform. Briefly, 2x10<sup>5</sup> cells, per well/90µL in a 96-well round bottom plate, are treated with 10 µL of 3-fold serial compound dilutions, starting at 30µM. The final vehicle concentration is 0.3% DMSO in all wells. After 24h incubation, cell pellet lysis is achieved by addition of 100µL MSD-lysis buffer/well and incubation on ice for 20 min. Inhibition of target cleavage is then assessed by transferring 50µL of lysate to the MSD plate pre-coated with anti-uncleaved BCL10 rabbit mAb (EP606Y/ab33905, Abcam). After 2h of incubation at RT, wells are exposed for 1h to an anti-BCL10 mAb (331.3/sc-5273, Santa Cruz Biotechnology). Immune complexes are detected by a SULFO-TAG™ anti-mouse secondary detection antibody incubated for 1 h at RT. Light emission at 620nm triggered by application of electric current is recorded on a MSD Sector Imager 6000. The effect of a particular test compound on Bcl10 cleavage inhibition is expressed relative to the effect of Z-VRPR-FMK; set as 100%. EC50 values (µM) are determined using 4-parametric curve-fitting (XLfit4 software, V2.2.2).
  14. To monitor the selectivity of MALT1 inhibitors with respect to suppression of proliferation of OCI-Ly3 compared to BJAB cell models, cells were incubated with serially diluted compounds and viability determined after 72 hours by measuring cellular ATP using a Cell TiterGlo assay kit (Promega). The concentration (IC50) at which half-maximal reduction of ATP levels relative to vehicle-treated controls were achieved was calculated using 4-parametric curve-fitting (XLfit, V4.3.2) of the dose-response curves.
  15. Compound 17 was tested in dose-response mode up to 30 µM for receptors, transporters and enzymes. Activity on the following proteases was tested up to 100 µM (IC50 [µM]): caspase3 (46), cathepsins B (94), C (88), G (>100), K (57), L (51), S (99), trypsin (>100), chymotrypsin (>100), chymase (>100), factor VIIa (>100), IXa (>100), Xa (>100), XIa (>100), XIIa (>100), kallikrein5 (>100), 7 (>100), MT-SP1 (>100), neutrophil elastase (>100), elastase1 (>100), proteinase 3 (>100), thrombin (>100), MMP8 (>100).
  16. Schlauderer F, Lammens K, Nagel D, et al. *Angew Chem Int Ed.* 2013;52:10384.
  17. Rat PK determination was performed using either cassette dosing or one-in-one experiments in permanently cannulated rats. Up to 7 compounds were dosed simultaneously at 1.0 mg/kg, i.v., in N-methyl-2-pyrrolidone, polyethylene glycol 200 (30%, 70%), and at 3.0 mg/kg, p.o. as suspension in carboxymethylcellulose, water, Tween80, (0.5%, 99%, 0.5%). Upon re-analysis the acid fragment could be detected in circulation in significant concentrations in several PK experiments from this compound series.
  18. Di L, Keefer C, Scott DO, et al. *Eur J Med Chem.* 2012;57:441.
  19. For a recent review see: Maiti D, Fors B, Henderson JL, Nakamura Y, Buchwald SL. *Chem Sci.* 2011;2:57.